Wei et al. Chemistry Central Journal 2012, 6:29
http://journal.chemistrycentral.com/content/6/1/29

Chemistry Central Journal

RESEARCH ARTICLE Open Access

Characterization of the 1st and 2nd EF-hands of NADPH oxidase 5 by fluorescence, isothermal titration calorimetry, and circular dichroism

Chin-Chuan Wei[1*], Nicole Reynolds[1], Christina Palka[2], Kristen Wetherell[1], Tiffany Boyle[1], Ya-Ping Yang[3], Zhi-Qiang Wang[4] and Dennis J Stuehr[3]

Abstract

Background: Superoxide generated by non-phagocytic NADPH oxidases (NOXs) is of growing importance for physiology and pathobiology. The calcium binding domain (CaBD) of NOX5 contains four EF-hands, each binding one calcium ion. To better understand the metal binding properties of the 1st and 2nd EF-hands, we characterized the N-terminal half of CaBD (NCaBD) and its calcium-binding knockout mutants.

Results: The isothermal titration calorimetry measurement for NCaBD reveals that the calcium binding of two EF-hands are loosely associated with each other and can be treated as independent binding events. However, the Ca^{2+} binding studies on NCaBD(E31Q) and NCaBD(E63Q) showed their binding constants to be 6.5×10^5 and 5.0×10^2 M^{-1} with ΔHs of -14 and -4 kJ/mol, respectively, suggesting that intrinsic calcium binding for the 1st non-canonical EF-hand is largely enhanced by the binding of Ca^{2+} to the 2nd canonical EF-hand. The fluorescence quenching and CD spectra support a conformational change upon Ca^{2+} binding, which changes Trp residues toward a more non-polar and exposed environment and also increases its α-helix secondary structure content. All measurements exclude Mg^{2+}-binding in NCaBD.

Conclusions: We demonstrated that the 1st non-canonical EF-hand of NOX5 has very weak Ca^{2+} binding affinity compared with the 2nd canonical EF-hand. Both EF-hands interact with each other in a cooperative manner to enhance their Ca^{2+} binding affinity. Our characterization reveals that the two EF-hands in the N-terminal NOX5 are Ca^{2+} specific.

Graphical abstract

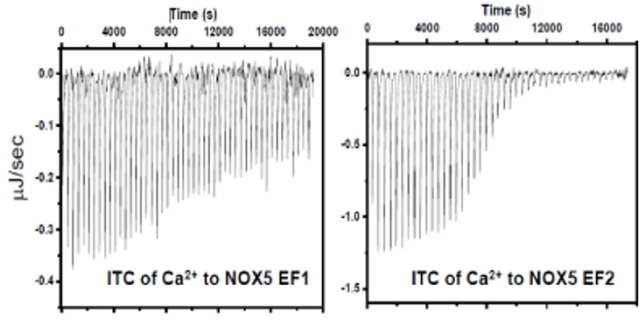

* Correspondence: cwei@siue.edu
[1]Department of Chemistry, Southern Illinois University Edwardsville, Edwardsville, IL 62026, USA
Full list of author information is available at the end of the article

Keywords: EF-hand, Calcium binding, NADPH Oxidase 5, Fluorescence, Isothermal titration calorimetry

Background

Reactive oxygen species (ROS), such as superoxide and hydrogen peroxide, play important roles in host defense, signal transduction, and hormone synthesis [1]. Superoxide is primarily generated by the enzyme family of NADPH oxidases (NOXs), and several homologous enzymes have been identified, including NOX1, NOX2, NOX3, NOX4, NOX5, and dual oxidase (DUOX) [2,3]. Among them, NOX2 (a.k.a. phagocyte NOX) serves primarily in nonspecific immunity by generating superoxide which kills invading microbes [4]. While a large amount of superoxide is essential in phagocytic cells, trace amounts of superoxide generated from other NOX enzymes are required for non-phagocytic cells to function properly. Accordingly, deficiency or overproduction of superoxide has been demonstrated to lead to pathological problems, as well as neurological, cardiovascular, and renal diseases.

The exact biological functions and superoxide-generating mechanisms for non-phagocytic NOXs are largely unknown. In phagocytes, two transmembrane proteins ($gp91^{phox}$ and $p22^{phox}$) interact with each other to form a stable core enzyme, flavocytochrome b_{558}. Upon stimulation by various agents, three additional protein components from the cytosol ($p47^{phox}$, $p67^{phox}$, and $p40^{phox}$) translocate to the membrane surface to form an active NADPH oxidase complex for superoxide production. Superoxide generated by this system is regulated by GTPases including Rac1, Rac2, and Rap1A. It has been shown that some non-phagocytic NOXs, such as NOX1 and NOX3, are regulated in a similar fashion as NOX2. Their activities are regulated by accessory proteins, such as NOXA1, $p47^{phox}$ and/or $p67^{phox}$ [2]. All NOX enzymes identified thus far show a sequence homologous to $gp91^{phox}$ in that they all contain a transmembrane cytochrome b-type heme domain linked to a NADPH-and FAD-flavoprotein domain. But NOX5, DUOX, and plant Rboh contain an additional EF-hand domain and their ROS-generating activity is directly mediated by Ca^{2+} flux. It appears that their EF-hands interact with their own heme and/or flavoprotein domains, allowing electron transfer to the molecular oxygen receiver. In NOX5, the EF-hand containing domain, or calcium binding domain (CaBD), interacts specifically with two peptide sequences within its flavoprotein domain in a Ca^{2+} dependent manner [5], which suggests that a domain-domain interaction is essential for NOX5-superoxide generating activity. The mechanism of how electron transfer is controlled by Ca^{2+} is still unclear. CaBD contains one non-canonical and three canonical EF-hand motifs (helix-loop-helix) with each one binding one Ca^{2+} ion (Figure 1A).

Using flow dialysis, Banfi *et al*. determined the macroscopic (stoichiometric) binding constants and derived their intrinsic binding constants (K_a) for the binding of the 1^{st} - 4^{th} Ca^{2+} ions to CaBD assuming independent binding among Ca^{2+} binding sites [6]. They concluded that the N-terminal half (NCaBD), containing the 1^{st} and 2^{nd} EF-hand (EF1 and EF2) motifs, has a lower calcium binding affinity, with K_a values ranging from 1.7×10^4 to 6.8×10^4 M^{-1}, while the C-terminal half (CCaBD), containing the 3^{rd} and 4^{th} EF-hand motifs, has a high calcium binding with K_a values ranging from 1.6×10^5 to 9.5×10^5 M^{-1}. They then demonstrated that the two halves functions independently in terms of Ca^{2+} binding affinities. Previously, we have shown that the higher Ca^{2+} affinity of the C-terminal half might be attributed to its slower Ca^{2+} dissociation using full-length CaBD and a mutant (CaBD (E99Q/E143Q)) in which the Ca^{2+} binding of EF3 and EF4 is impaired [7]. Further, our data suggest that the two halves have different metal binding properties. To ambiguously confirm our previous conclusion about the N-terminal half of CaBD, which require excluding the contribution of Trp fluorescence and secondary structural change from the C-terminal half, we specifically generated the recombinant N-terminal half of CaBD and its mutants, and separately studied their metal binding using fluorescence, isothermal titration calorimetry, and circular dichroism. Our results supported our previous findings about the different metal binding characteristics and revealed a possible mechanism for Ca^{2+} binding to the 1^{st} and 2^{nd} EF-hands of NOX5. The binding thermodynamic parameter, such as enthalpy difference (ΔH), and structural change for Ca^{2+} binding are also presented.

Results and discussion

Effects of metal ions on trp fluorescence of NCaBD and its mutants

The measurement of Ca^{2+} binding to NCaBD by fluorescence is possible because it contains two Trp residues (W9 and W12) at its N-terminal end. Upon the addition of Ca^{2+}, the fluorescence of NCaBD enhanced ~38% and its maximum emission wavelength shifts slightly from 352 nm to 354 nm (upper panel in Figure 2A). This calcium-induced fluorescence change is unexpected because a previous report by Banfi et al. showed that its fluorescence was not affected by Ca^{2+} binding [6]. The reasons for such spectroscopic discrepancy is not clear, but it may be due to differences in protein preparation, such as the additional N-terminal His residues present in our protein construct whereas a fused glutathione transferase (GST) was used in their protein construct. The Ca^{2+} titration to

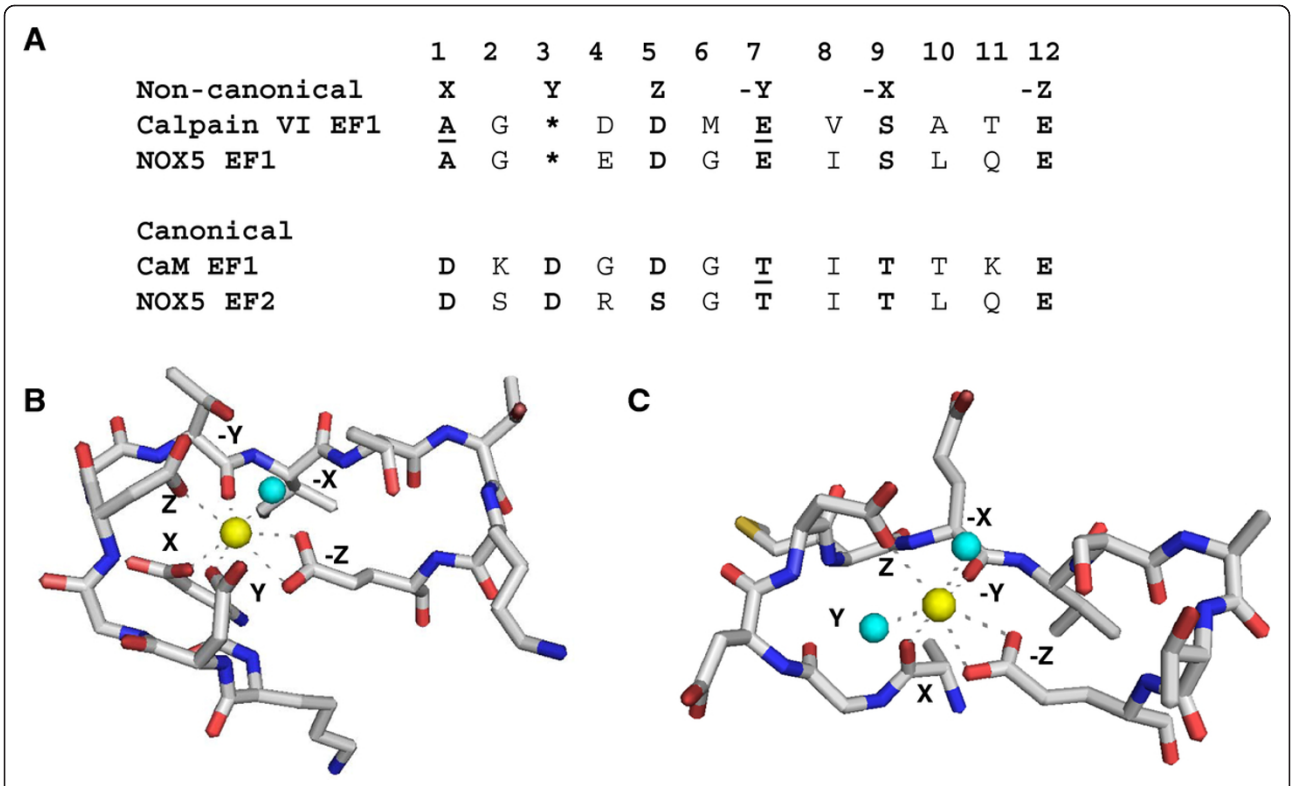

Figure 1 The non-canonical and canonical EF-loops. The sequences comparisons of NOX5's EF1 and EF2 to the preventative non-canonical calpain V1 EF1and canonical CaM EF1 is presented in **A**, where the Ca^{2+} ligands provided by the carbonyl group of backbone is underlined. The crystal structure of the EF-loop of CaM EF1 (PDB: 1XER) indicates a canonical arrangement (**B**) where the structure of the EF-loop of calpain V1 EF1 (PDB: 1DVI) indicates a non-canonical arrangement (**C**). The Ca^{2+} ions and water molecules are presented as yellow and cyanine spheres, respectively. The figure is created using PyMol (Molecular Graphics System, Schrönger LLC).

NCaBD revealed a negative cooperative binding with the value of the Hill constant (n_H) equaling 0.9 (lower panel in Figure 2A).

To better understand what role the individual EF-hands in NCaBD play in metal binding, we generated three mutants, NCaBD(E31Q), NCaBD(E63Q) and NCaBD(E31Q/E63Q), in which the Glu residues at the -Z (+12) position of the corresponding EF-hands were replaced with Gln. Such mutation approach has been employed to impair calcium binding affinity in NOX5 [6,7] and other Ca^{2+} binding proteins [8]. In order to better associate Ca^{2+} binding with the individual EF-hands, we refer to NCaBD(E31Q) as -1EF+2EF to emphasize that its Ca^{2+} binding site at the 1st EF-hand is "removed" while the 2nd EF-hand is intact. Similarly, NCaBD(E63Q) and NCaBD(E31Q/E63Q) are referred as +1EF-2EF and -1EF-2EF, respectively. The fluorescence of -1EF+2EF enhances ~20% upon Ca^{2+} binding and 50 μM Ca^{2+} is enough to saturate the binding (data not shown). The fluorescence of +1EF-2EF was also enhanced ~20% upon Ca^{2+} binding (upper panel in Figure 2B). Interestingly, its binding is very weak; approximately 4 mM Ca^{2+} was required to saturate the binding. Since ITC provides more binding characteristics than fluorescence, we used it to determine the Ca^{2+} binding constants and the corresponding thermodynamic parameters. However the lower Ca^{2+} affinity of +1EF-2EF allowed us to perform a direct titration using fluorescence since the free Ca^{2+} concentration is roughly equal to the total Ca^{2+} concentration for a weak binding. The titration revealed that its Ca^{2+} binding is best fitted with cooperative binding (n_H = 1.50) (lower panel in Figure 2B). Note that the observed binding constant, $K_{obs,}$ obtained from Hill equation is not related to either macroscopic or microscopic binding constant. We used a model with two binding sites and determine its K_a values to be 6.1×10^2 and 2.2×10^2 M^{-1} (data not shown). The fluorescence titration indicates that the mutated EF2 still retains its Ca^{2+}-binding ability, albeit much weaker, which is affected by the Ca^{2+}-bound EF1 in a positive cooperative manner. By combining the measurement from ITC (see below), we estimated K_a for EF1 to be ~ 5×10^2 M^{-1}. The double mutant, -1EF-2EF, showed no response to Ca^{2+} up to 20 mM, indicating that replacing Glu with Gln has completely abolished Ca^{2+} binding for all EF-hands. Measurements with Ca^{2+} concentration higher than 20 mM Ca^{2+} poses difficulties

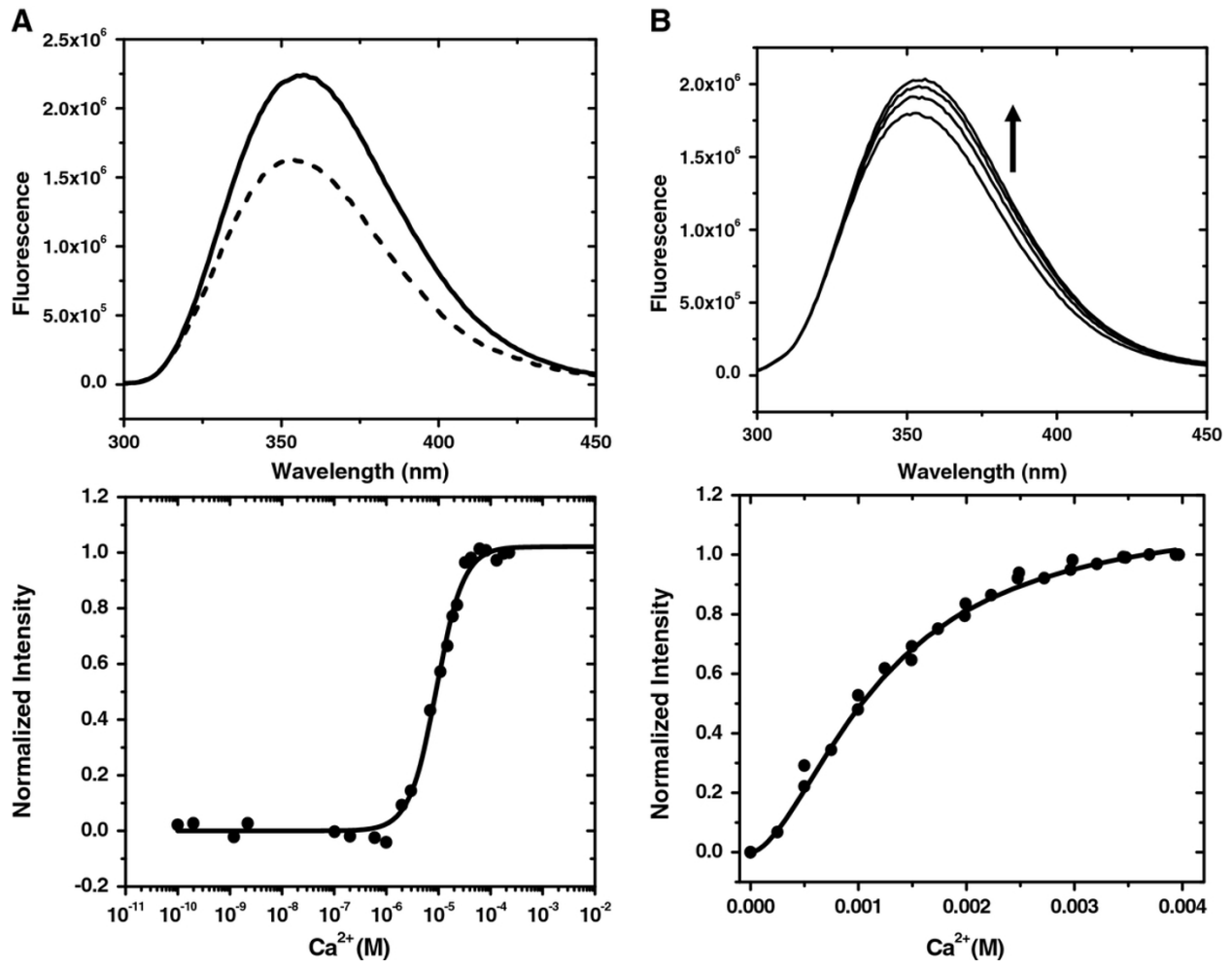

Figure 2 Fluorescence and Ca^{2+} binding of NCaBD and +1EF-2EF. A solution containing 4 μM NCaBD was excited at 280 nm and the emission spectra was recorded at 20°C in the presence of 500 μM EDTA (dotted line) and 100 μM Ca^{2+} (solid line) **(upper panel in A)**. Solutions of different Ca^{2+} concentrations were titrated to a solution containing 2 μM NCaBD and the emission intensities were recorded at 350 nm. The normalized fluorescence was fitted with a Hill equation with n = 0.91 **(lower panel in A)**. Ca^{2+} binding to +1EF-2EF was monitored by fluorescence with an excitation at 280 nm. The intensity enhanced with 1 mM Ca^{2+} interval and leveled off at 3-4 mM Ca^{2+} **(upper panel in B)**. The titration monitored at the emission intensity of λ_{350} nm fit a model with a Hill equation **(lower panel in B)**. Data shown are representative of at least four independent experiments.

because it decreases fluorescence intensity as protein solubility decreases and ionic quenching occurs. Thus, replacing Glu to Gln at both EF-hands results in very weak Ca^{2+} binding (< 50 M^{-1}), which is not biologically significant.

Previously, we characterized the AEDANS labeled CaBD and CaBD(E99Q/E143Q), in which the fluorescent dye is labeled at cys-107 that is located in EF3 and EF4. The labeled proteins are believed to be more sensitive to the structural change of the C-terminal half and our data suggest that only the C-terminus half of CaBD binds to Mg^{2+} [7]. We included up to 20 mM Mg^{2+} to the wild type and the mutants of the N-terminal half domain but no significant fluorescence change was observed, thus confirming our previous conclusion.

Stern-Volmer quenching

We employed fluorescence quenching to differentiate between the structures of Ca^{2+}-bound and apo NCaBD by determining the accessibility of Trp residues to acrylamide. Fluorescence decrease is the result of Trp either being translocated to the surface of the protein or of Trp being located in the interior of a protein channel that acrylamide is able to diffuse into. The Trp residue(s) were more accessible for quenching in the calcium-bound form (K_{sv} = 12.66 M^{-1}) than the apo form (K_{sv} = 6.95 M^{-1}) (Table 1). Ca^{2+} binding has a similar effect on Trp accessibility for +1EF-2EF and -1EF+2EF though their K_{sv} values are lower than the wild type. These results, together with direct fluorescence titration, suggest the environment of the Trp residues located in the

Table 1 Stern-Volmer Quenching Constants Obtained from Acrylamide Titration

	K_{sv} (M^{-1})		
Protein	apo	Mg^{2+}	Ca^{2+}
CaBD	5.28 ± 0.22	5.04 ± 0.35	9.49 ± 0.52
NCaBD[a]	6.95 ± 0.22	6.78 ± 0.35	12.66 ± 0.52
-1EF+2EF[a]	6.61 ± 0.17	6.68 ± 0.33	9.28 ± 0.08
+1EF-2EF[a]	6.70 ± 0.21	6.71 ± 0.15	9.51 ± 0.16
-1EF-2EF[a]	7.40 ± 0.42	7.35 ± 0.35	7.45 ± 0.41

[a]Proteins were excited at 280 nm and their intensities at the maximum wavelengths were recorded. The concentrations of EDTA, Mg^{2+}, and Ca^{2+} were 0.5, 10, and 1 mM (4 and 10 mM for +1EF-2EF and -1EF-2EF, respectively).

N-terminal end is altered by Ca^{2+} binding to EF1, EF2, or both. We did not see any quenching change for -1EF-2EF in the presence of Ca^{2+}. In agreement with fluorescence titration, no significant quenching change was observed in the presence of Mg^{2+} for the wild type and mutants.

Secondary structures determined by circular dichroism

The characterization by fluorescence and fluorescence quenching clearly suggests that Ca^{2+}, but not Mg^{2+}, binds to all protein constructs except -1EF-2EF. To eliminate the artifacts that possibly arise from a structural change caused by the Glu→Gln mutation, we monitored all constructs in the absence of Ca^{2+}. The CD spectrum of NCaBD shows two negative elliptical peaks near 208 and 222 nm and one large positive band at 190 nm (Figure 3), which are characteristic peaks of proteins containing a dominate α-helical secondary structure. All mutants had identical CD spectra, indicating that such a mutation does not alter structural integrity. The addition of Ca^{2+} to NCaBD significantly changes the CD signal by increasing the content of α helix. Ca^{2+} also induces additional α helix formation in +1EF-2EF and -EF+2EF, but to a smaller extent (data not shown). In the presence of Mg^{2+}, no significant conformational change was observed for all proteins.

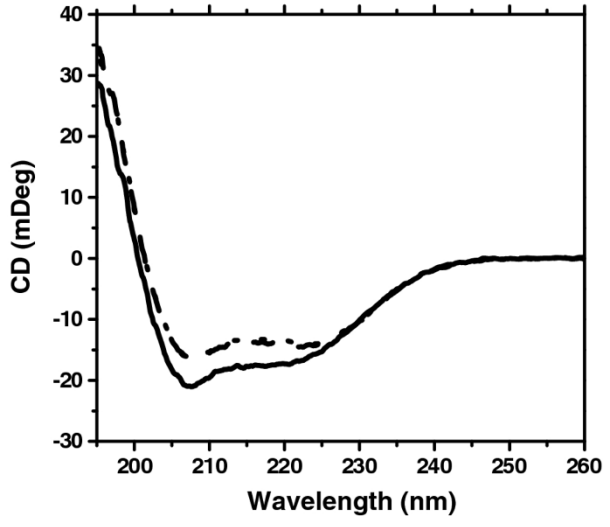

Figure 3 CD Spectra of NCaBD. Spectra were recorded at 20°C in 10 mM Tris, pH 7.5 in the presence of 500 μM EDTA (dotted line) and 1 mM Ca^{2+} (solid line). Data shown are representative of three independent experiments.

Isothermal titration calorimetry

The ITC thermogram exhibits a typical calorimetric reaction upon the addition of aliquots of Ca^{2+} to NCaBD (upper panel in Figure 4A), in which the heat evolved per injection increased in the presence of low Ca^{2+} concentration and then decreased when the molar ratio reached 1.5. The heat evolved decreased gradually till the background signal was reached. The plot of heat evolved per injection (ΔQ_i) versus molar ratio is showed in the lower panel of Figure 4A. The ITC data can not be fit to a model with one (type) binding site. Since there is no information regarding the sequential Ca^{2+} binding in NOX5, it is very important to analyze the ITC data carefully due to this featureless ITC thermogram. As shown in other EF-containing proteins, Ca^{2+} binding in one EF-hand might affect the Ca^{2+} binding to the other EF-hand. Thus, we treated our data with a binding polynomial formula, assuming nothing about the presence or absence of cooperativity [9,10]. Nonlinear least squares analysis yielded overall association constants, βs, and the associated enthalpy changes (ΔHs) for one and two Ca^{2+} ions binding to NCaBD: $\beta_1 = 2.90 \times 10^6\ M^{-1}$, ΔH_1 = -4.86 kJ/mol, $\beta_2 = 4.86 \times 10^{11}\ M^{-1}$, and ΔH_2 = -28.73 kJ/mol. The macroscopic cooperative constant ρ was then determined to be 0.333 ($\rho = 4\beta_2/\beta_1^2$), which indicates that the binding model is either two independent binding sites or two identical binding sites with a negative cooperativity. If a cooperative model is used, the cooperative Gibbs energy difference is +2.6 kJ/mol (+0.68 kcal/mol). The free energy penalty posted by this negative cooperative binding is relatively small, indicating that the binding affinity of the 2^{nd} Ca^{2+} ion is slightly decreased when the first Ca^{2+} ion occupies either of the two binding sites. Using a model with two non-identical sites fits our ITC data equally well with integer stoichiometry (n_1 = 0.9 and n_2 = 1.1); the values of K_a and ΔH were determined to be $8.6 \times 10^6\ M^{-1}$ and -4.96 kJ/mol and $3.05 \times 10^5\ M^{-1}$ and -24.88 kJ/mole for the two EF-hands. In this model, the determined binding affinity constants become intrinsic binding constants for the individual EF-hands. The intrinsic binding constants determined from this study are at least one order stronger than the reported values, and the affinity of one of binding site is stronger than the other by a factor of 30 (Table 2). The ITC measurement also indicates that the 1^{st} Ca^{2+} binding is an entropy-driven interaction due to a small ΔH (~ -4 kJ/mol) while

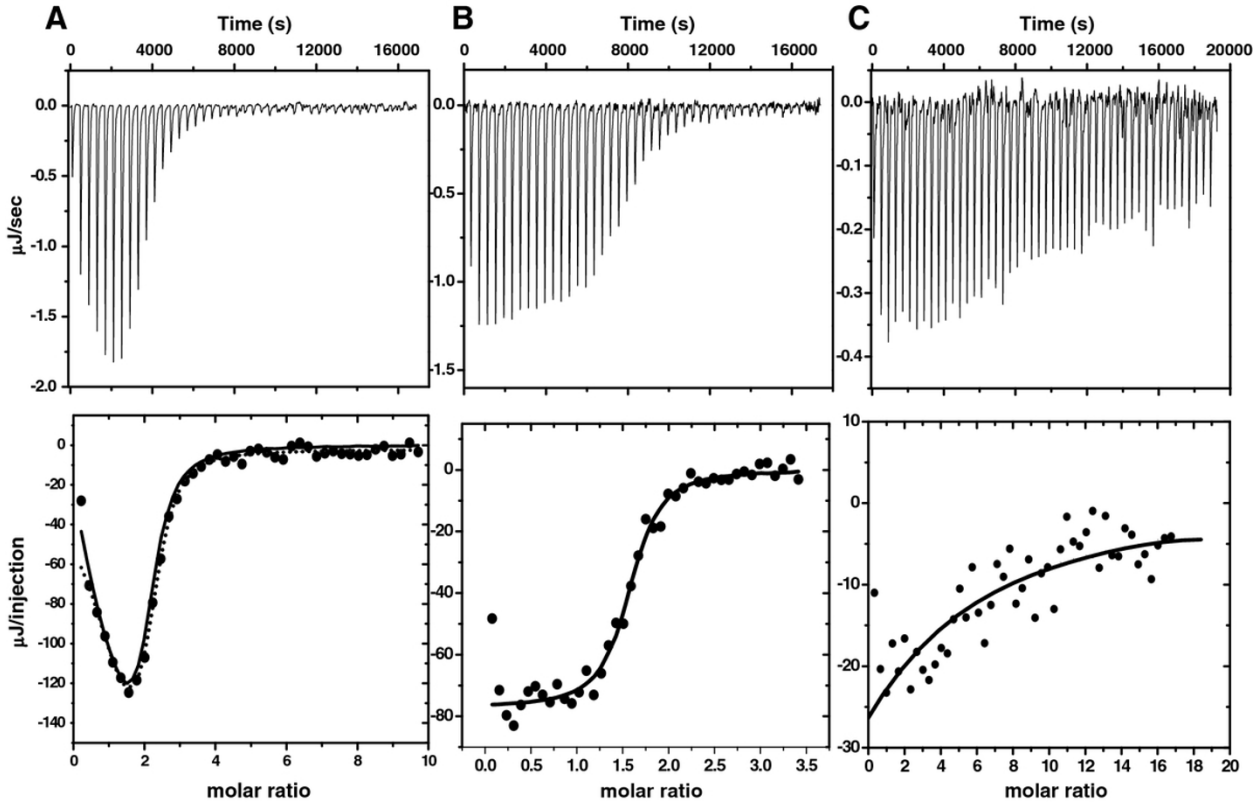

Figure 4 Binding of Ca^{2+} to NCaBD, -1EF+2EF, and +1EF-2EF as measured by ITC. For each injection, 2-µL of a 3-mM Ca^{2+} solution was mixed in a sample cell containing 37.5 µM NCaBD **(upper panel in A)** or 75 µM -1EF+2EF **(upper panel in B)** at 25°C. The heat evolved was recorded during titration. The corrected heats evolved per injection for NCaBD was either fitted to a model with 2 independent binding sites (solid line) or with a model with identical, cooperative binding sites (dashed line) **(lower panel in A)**. The ITC thermogram of -1EF+2EF was fitted with a model to one binding site **(lower panel in B)**. A solution of 30 mM Ca^{2+} was titrated into 75 µM +1EF-2EF and its resulting heat evolved per injection was recorded **(upper panel in C)**. The corrected ITC data was fitted with a single (type) binding site model **(lower panel in C)**. The first point in ITC titration was not included in fitting. Data shown are representative of at least four independent experiments.

the 2nd Ca^{2+}-binding is more likely an enthalpy-driven interaction ($\Delta H = \Delta H_2 - \Delta H_1 = \sim -24$ kJ/mol). The binding isotherm is reproducible when a higher concentration of protein was used, which exemplifies the heat evolved in the lower molar ratio of [Ca^{2+}]/[NCaBD] (see Additional file 1: Figure S1).

As expected, the Ca^{2+} titration of -1EF+2EF measured by ITC can be fit to a model with one binding site and yielded the values of K_a and ΔH to be 6.5×10^5 M^{-1} and -14.1 kJ/mol, respectively (Figure 4B). The heat released due to Ca^{2+} binding to EF2 alone is between the ΔH values for the 1st and 2nd Ca^{2+} binding, suggesting that the model with independent binding is unlikely. The binding affinity of EF2 is comparable to the values derived from the ITC analysis of NCaBD. For +1EF-2EF, the signal to noise ratio (S/N) of the ITC signal was too

Table 2 The Ca^{2+} Binding constants for the 1st and 2nd EF-hands

Protein	K_a M^{-1} (ΔH kJ/mol)
NCaBD[a]	1.7 -6.8×10^4
NCaBD[b]	$3.05 \pm 1.02 \times 10^5$ (-4.96 ± 0.25), $8.60 \pm 1.65 \times 10^6$ (-24.88 ± 0.43)
-1EF + 2EF	$6.51 \pm 0.80 \times 10^5$ (-14.3 ± 0.3)
+1EF-2EF [c]	$\sim 5 \times 10^2$ (-4.0 ± 0.2)
-1EF-2EF	N/D[d]

[a]The data is from ref. [6].

[b]The ITC data was fitted with a model with two independent binding sites.

[c]The binding constant was estimated from fluorescence and ITC, assuming two Ca^{2+} binding sites.

[d]Not detected.

small to make a precise determination of its binding constant (Figure 4C). The K_a value was estimated to be ~800 M^{-1} for one-binding site or ~400 M^{-1} for two identical binding sites, which is consistent with the value determined from fluorescence characterization (Figure 2B). The value of ΔH was calculated to either -8 kJ/mol for a model with one binding site or -4 kJ/mol for a model with two identical binding sites. Total heat generated for Ca^{2+} binding to +1EF-2EF was further confirmed using a separate continuous titration method that determines ΔH directly (data not shown).

Although Mg^{2+} binding was not observed in our spectroscopic study, one can not completely rule out the possibility since the Trp fluorescence or CD only reflects the change on Trp residue(s) or the secondary content change, respectively. For example, the C-terminal half of CaBD contains one Trp residue that is distant from its EF-hands and does not change its Trp fluorescence upon Ca^{2+} binding (ref. [6] and our unpublished result). Mg^{2+} binding most likely changes only local structures, enabling no significant signal in CD and fluorescence. Because it is not possible to extract useful binding parameters using a direct ITC titration for a low Mg^{2+} binding, we performed a competitive ITC binding experiment by titrating Ca^{2+} to a solution containing the protein plus 20 mM Mg^{2+}. If Mg^{2+} does bind to our proteins, the additional Ca^{2+} ions has to compete with the same binding site(s) occupied by Mg^{2+}, resulting in lower binding affinity. We have not observed any ITC binding change.

Previously, we generated a CaBD mutant, (E99Q/E143Q) or +1EF+2EF-3EF-4EF [7], which presumably functions as NCaBD. To check if this is the case, we thus measured its Ca^{2+} binding by ITC. We observed an identical binding isotherm as that of NCaBD (data not shown) and the results also indicate that replacing Glu with Gln in EF3 and EF4 does impair their Ca^{2+} binding significantly.

Conclusion

The process by which Ca^{2+} induces conformational change in NOX5's CaBD is critical for the inter domain-domain interaction and is required in order to produce superoxide. The interaction appears to be mediated by the four EF-hands it contains. In the past decade, characterization of a variety of calcium binding proteins provides a wealth of information about how Ca^{2+} binding to their individual EF-hands leads to biological responses. However, it is impossible to predict Ca^{2+} binding strength and its cooperativity simply based on the sequences of EF-loop because the Ca^{2+} binding is dependent upon the overall structure not simply the loop change [11]. The characterization of the non-canonical EF1 and canonical EF2 reveals that Ca^{2+} binding to NCaBD induces a structural change as observed in the enhancement of Trp fluorescence and the increase of α secondary structure. The Trp fluorescence results show that λ_{max} is shifted from 340 in CaBD to 350 nm in NCaBD upon Ca^{2+} binding, suggesting that the red spectrum shift is caused by Trp residues being more exposed to solvent when the C-terminal half is not present. This explains equally well the higher K_{sv} values for the apo NCaBD than the apo CaBD and the Ca^{2+}-bound NCaBD than Ca^{2+}-bound CaBD that were observed (Table 1).

Data analysis of Ca^{2+} binding affinities to NCaBD obtained by ITC titration indicates that the Ca^{2+} binding to EF1 and EF2 could be explained by a model with two independent binding sites or identical intrinsic binding with a slightly negative cooperative. The data is somewhat parallel to the flow dialysis data that assume no interaction between EF-hands and, thus, the corresponding intrinsic binding constants were derived by statistics. However, analysis using either model provides no information about the Ca^{2+} binding for each EF-hand. Given a very weak macroscopic cooperative binding as observed in NCaBD, it is fair to assume that NCaBD contains a non-interacting pair of EF-hands, which is in agreement with the assumption made in a previous report using Adair equation [6]. However, our ITC data clearly indicates that the macroscopic and microscopic binding constants for NCaBD, assuming an independent model, are one-order higher than the reported values, and also the binding for one site is one order stronger than the other (Table 2).

While there is no indication that individual EF-hands interact with each other due to the fact that the ITC and fluorescence studies of Ca^{2+} binding to NCaBD could only provide macroscopic view of Ca^{2+} binding, mutagenesis studies on individual EF-hands do indicate that this independent binding model is unlikely. The NOX5's 2nd EF-loop has a conserved canonical EF-hand sequence (Figure 1A) and also shows a strong Ca^{2+} binding (K_a = ~ 10^6 M^{-1}), suggesting its Ca^{2+} model is similar to known canonical EF-hands by chelating Ca^{2+} to the residues at +X (1), +Y (3), +Z (5), -Y (7), and -Z (12) with a water molecule through the residue at -X (9) (Figure 1B). The non-canonical EF1 alone has a very weak Ca^{2+} binding with a ΔH value of -4 kJ/mol. Because CD and quenching studies indicate there is no structural difference between the wild type and mutants in the absence of Ca^{2+}, the low Ca^{2+} binding affinity of EF1 could not simply be explained by structural alternation due to mutation. The EF-loop of EF1 contains only 11 amino acids with non-prototypic acid residues in +X and +Y positions, which is found in most members of the penta-EF-hand superfamily such as sorcin, calpain, and grancalcin. Although the binding affinity of non-canonical EF-hands is not necessarily weaker than canonical EF-hands, the low binding affinity of EF1 might be

attributed to the decrease in entropic contribution. In caplain domain VI (dVI) the non-canonical EF1 (Figure 1C), which shares similar sequence to NOX5' EF1, adopts an alternative conformation by chelating Ca^{2+} to the oxygen molecule of a main-chain carbonyl group (+X) and to an additional water molecule (+Y) [12,13]. Thus with two "frozen" water ligands remaining within EF-loop, the affinity is decreased. Thus our data suggests that in order for NOX5 EF1 to adopt an optimal conformation for Ca^{2+} binding, the structural change on EF2 upon Ca^{2+} binding is essential to increase its sensitivity.

We propose a possible model for Ca^{2+} binding to NCaBD (Figure 5). The intrinsic Ca^{2+} binding constants (K_I and K_{II} for EF1 and EF2, respectively) are determined by using +1EF-2EF and - 1EF+2EF. The data analysis from the ITC data of NCaBD determines the overall binding constant (β_j) or stepwise binding constant (K_j) for ligation of the j^{th} site (see Experimental Section). Because the thermodynamics is independent of the reaction pathway, the equation $\beta_2 = K_I \times K_{II,I} = K_{II} \times K_{I,II}$ is upheld where $K_{I,II}$ is intrinsic Ca^{2+} binding constant for EF1 in the presence of Ca^{2+}-bound EF2. Thus the microscopic cooperative constant (c_{12}) is determined by the definition of $K_{I,II}/K_I$ or $K_{II,I}/K_{II}$. For NCaBD, Ca^{2+} first binds to EF2, the higher Ca^{2+} binding affinity site. The resulting binding causes a conformational change that propagates to EF1, thus enhancing its Ca^{2+} binding, in which c_{12} is estimated to be ~ 1,500. In other words, it implies that microscopic cooperativity occurs in NCaBD, which is masked by macroscopic cooperativity [14]. Future studies using NMR spectroscopy which determines Ca^{2+} binding in both EF-hands simultaneously should reveal the steps in the transition from apo state to holo state and determine the microscopic cooperativity precisely [15].

It is believed that Mg^{2+} binding to EF-hands is biologically important. EF-hands bind to Mg^{2+} in a substantially different way than Ca^{2+}; it causes conformational change locally and is unable to elicit enzymatic activity. In the resting cells, the concentration of Mg^{2+} is 0.5-2 mM and thus it is a potent competitor for EF-hands. Here, we concluded unambiguously that Mg^{2+} binding to NCaBD is not biologically important. To our best knowledge, there is no report of Mg^{2+} binding to non-canonical EF-hands. For canonical EF-hands, an acid-pair theory, which states that the strength of Mg^{2+} binding is proportional to the numbers of X, Y, Z acid pairs (i.e. the X-acidic pair contains two acidic residues, Asp or Glu, in +X and -X positions), has been used to explain Mg^{2+} binding affinity [16]. In agreement with this theory, the NOX5's EF2 contains no acidic pairs and shows no Mg^{2+} binding.

Ca^{2+} binding to NOX5 was determined to be weak and, because of this, a question arises concerning whether the Ca^{2+} level (~10^{-5} M) in activated cells is able to saturate and activate NOX5. Here, we show that NOX5's EF1 and EF2 possess a higher binding affinity than the reported values. Our preliminary results indicate that Ca^{2+} binding to CaBD gates heme reduction using membrane solublized NOX5 and enhances the electron transfer from NADPH to FAD in the flavoprotein domain, which was determined using cytochrome C assay (unpublished results). We are investigating how the individual EF-hands impact on the

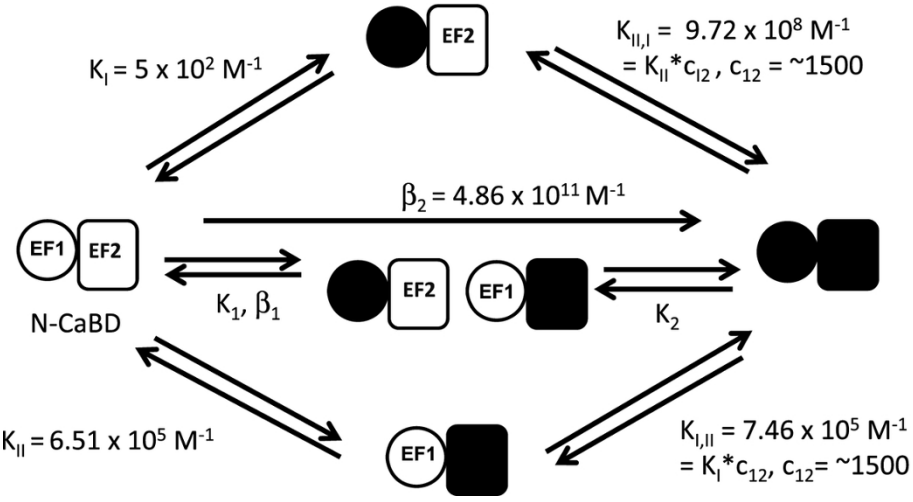

Figure 5 A proposed model for Ca^{2+} binding to NOX5's EF1 and EF2. A microscopic binding model is proposed based on the studies of -1EF+2EF and +1EF-2EF that determine their microscopic binding constants (k_I and k_{II} for EF1 and EF2) and the studies of NCaBD that determine their overall binding constants, β_1 and β_2. Due to the equilibrium among all states, the equation $\beta_2 = K_I \times K_{II,I} = K_{II} \times K_{I,II}$ was used to determine intrinsic binding constants of EF1 in the presence of Ca^{2+}-bound EF2 ($K_{I,II}$) and of EF2 in the presence of Ca^{2+}-bound EF1 ($K_{I,II}$). The microscopic cooperativity constant, c_{12}, was determined by the equation: $c_{12} = K_{II,I}/K_{II} = K_{I,II}/K_I$.

NOX5 superoxide-generating activity. Recent studies indicate that NOX5's calcium sensitivity is enhanced when its flavoprotein domain interacts with CaM [17] or is phosphorylated at its Thr494 and Ser498 residues [18]. All evidence suggests that the elevation of Ca^{2+} flux is critical for NOX5 activation while other factors further regulate its superoxide-generating activity. Because the activation still relies on Ca^{2+} binding, exactly how the structural change in the C-terminal flavoprotein is induced by the above mechanisms and propagates to CaBD remains to be studied further. Studies examining Ca^{2+} binding to individual NOX5's EF-hands are important for further elucidation of the mechanism.

Experimental

General

All chemicals were purchased from Sigma-Aldrich (St. Louis, MO) and Fisher Scientific, and were used without further purification. All buffers used in the protein characterization were rendered "calcium-free" by treatment with Chelex-100 (Bio-Rad Laboratories, Hercules, CA). The measurements were performed at least three times using at least three different protein batches, and the results were reproducible.

Plasmid constructions

The plasmid pLW-His_6-NCaBD (residues 1-78) was generated as described previously [7]. All constructs contain an extra 11 residues, MAHHHHHHAVP, at their N-terminal ends. The mutants NCaBD(E31Q), NCaBD(E63Q) and NCaBD(E31Q/E63Q) were created using the PFusion Mutation kit (New England Biolabs, Ipswich, MA). Polymerase chain reactions (PCRs) were performed using an Eppendorf MasterCycler ep thermocycler (Hauppauge, NY). The oligonucleotides for PCR were synthesized by Integrated DNA Technologies (Coralville, IA). The desired mutations in plasmid constructs were confirmed either by DNA sequencing or silent-digestion.

Recombinant protein expression and purification

The protein expression was performed as described previously [7]. In general, T7 *E. Coli* cells (New England Biolabs) carrying the desired plasmid were induced with 0.5 mM isopropyl β-D-1-thiogalactopyranoside (IPTG) at OD_{600} = 0.6-0.8 and the culture was continuously incubated for an additional 4-6 h at 37°C. Cells were then homogenized and the released His-tagged proteins were purified by chromatography. NCaBD was purified through a phenyl-sepharose column as described for NOX5's CaBD [7]. Mutants were first purified through a Ni-NTA column followed by a DEAE cellulose (Sigma-Aldrich) column (2.5 × 10 cm) using a BioLog FPLC System (Bio-Rad Laboratories). The flow rate was 1 mL/min. The DEAE column was equilibrated with a buffer containing 50 mM Tris, pH 7.5 (Buffer A) and the desired protein was eluted with a linear gradient from 0 to 100% Buffer B (50 mM Tris, pH 7.5, 0.3 M NaCl) over approximately 1.5 h. NCaBD(E31Q), NCaBD(E63Q), NCaBD(E31Q/E63Q) were eluted out at 54-69%, 50-65%, and 47-61% buffer B, respectively. To render the protein Ca^{2+}-free, an EDTA solution was added to the protein samples to make the final concentration of 5 mM followed by dialysis against a 1-L buffer containing 50 mM Tris, pH 7.5 and 1 mM EDTA overnight at 4°C. The proteins were then buffer-exchanged with Chelex-treated buffer in an Amicon Ultra centrifugal filter device (3,000 Da MWCO) or by gel filtration (Sephadex G-25). The purified proteins were stored at -80°C until use. The protein purity was checked on SDS electrophoresis and its purity was estimated > 90% based on density profiles measured using UN-SCAN-IT software (Silk Scientific, Inc, Utah). The SDS-PAGE picture of purified proteins used in this study is shown in Additional file 2: Figure S2. The protein concentration was estimated with the Bradford assay (Bio-Rad Laboratories) using bovine serum albumin (BSA) as standard.

Isothermal titration calorimetry

The ITC experiments were carried out on a Nano-ITC^{2G} instrument (TA instruments, DE) at 25°C. All samples were degassed before loading. The syringe and reaction cell were treated with a solution containing 100 μM EDTA to remove any residual Ca^{2+} followed by an exhaustive rinse of Chelex-treated water and buffer. A typical titration was performed by sequential injections every 400 s of 1.6 to 4 μL of a 3-5 mM Ca^{2+} (or 10-30 mM Mg^{2+}) solution into a hastelloy reaction cell (0.94 mL) that contained 0.0375-0.160 mM protein. The sample cell was stirred continuously at 200 rpm. Samples were re-examined for precipitation prior to and after titration. No precipitation was ever observed. The ITC raw data was corrected for the heat of titrant dilution determined by an experiment conducted in an identical condition except that there was no protein in the sample cell. Since TA Instruments use a positive sign for an exothermic reaction, which is opposite to the conventional presentation used by MicroCal (GE), we manually converted the measured raw data that are presented in all figures.

Spectroscopic measurements

Absorption measurements were carried out using a UV-1800 double-beam spectrometer (Shimadzu, Kyoto, Japan). The fluorescence spectra were recorded on a FluoroMax-3P (Horiba John Yvon, Inc.) equipped with excitation/emission polarizers and a temperature control unit. Since there is no Tyr residues in NCaBD, the Trp fluorescence spectra were obtained using 2-4 μM protein with an excitation wavelength of 280 nm at 20°C. The slit widths of 2 and 5 nm for excitation and emission,

respectively, were chosen to eliminate photobleaching. For Ca^{2+} titration, solutions of Ca^{2+} ranging from 1 M to 1 μM were added in increments of 1 and 2 μL to 1 mL of the protein solution. After each addition of Ca^{2+}, the sample was incubated for 1 min before measuring. All reported spectra were corrected for buffer effects, dilution factors, and any wavelength-dependent response for the fluorometer.

Stern-volmer quenching

Intrinsic Trp fluorescence quenching experiments were carried out at 20°C by adding a stock solution of 6 M acrylamide, which was determined using the absorbance coefficient ε_{295} = 0.25 M^{-1} cm^{-1} for acrylamide, to a sample solution containing 4-10 μM protein and 50 mM Tris, pH 7.5, 0.125 M NaCl, The following Stern-Volmer quenching equation was used for fitting:

$$F_o/F = (1 + K_{sv}[Q]) \quad (1)$$

where F and F_o are the fluorescence intensities at a given concentration of quencher (Q) and in the absence of quencher, respectively; K_{sv} is the dynamic or collisional quenching constant.

Far-UV circular dichroism (CD)

The CD spectra were recorded using a JASCO J-715 instrument (JASCO Corporation, Japan) at ambient temperature. Approximately 0.1 mg/mL protein in 10 mM Tris, pH 7.5 in the presence of EDTA, Mg^{2+}, or Ca^{2+} were placed in a cylindrical 0.1 cm path length quartz curve. All spectra were the average of 6 scans with a scan rate of 20 or 50 nm/min and were corrected by subtracting the spectra of buffers.

Data analysis

The titration data from fluorescence measurements were fitted with either a Hill equation or a model with one or two binding sites (n = 1 or 2) as in Eq. 2.

$$\Theta = \frac{F - F_{\min}}{F_{\max} - F_{\min}} = \sum_{i=1}^{n} \frac{([P]_t + [L] + 1/K_{ai}) - \sqrt{([P]_t + (L) + 1/K_{ai})^2 - 4[P]_t[L]}}{2[P]_t} \quad (2)$$

where Θ is the fraction of the ligand-bound protein; F_{max} and F_{min} are the maximum and minimum intensities during titration; F is the intensity at a specific ligand concentration; $[P]_t$ and [L] are the concentration of total protein and free ligand (in a weak binding, the concentration of free ligand is approximately equal to the concentration of total added ligand).

ITC measures heat evolved (Q) from the formation of ligand-protein complex. This binding constant(s) and its corresponding molar heat enthalpy (ΔH) for the reaction are calculated directly from the plot of heat evolved for each injection (ΔQi) versus molar ratio of ligand and protein using the software associated with ITC. We used NanoAnalyze (TA Instruments) to fit our data with one- independent, two-independent, or cooperative binding models.

NCaBD containing two Ca^{2+} binding sites will need to be fit with a two binding site model. The linkage for a model-free binding and a model-dependent binding is shown in Figure 5, where the relationship of macroscopic (stepwise or stoichimetric) binding constants (K_1 and K_2), overall binding constants (β_1 and β_2) and microscopic association biding constants, K_I and K_{II} is shown.

The stepwise and overall binding constants for Ca^{2+} binding to NCaBD are expressed as follows.

$$NCaBD + Ca^{2+} \leftrightarrow NCaBD/Ca^{2+} \qquad K_1 = \beta_1 = \frac{[NCaBD/Ca^{2+}]}{[NCaBD][Ca^{2+}]} \quad (3)$$

$$NCaBD/Ca^{2+} + Ca^{2+} \leftrightarrow NCaBD/2Ca^{2+} \qquad K_2 = \frac{[NCaBD/2Ca^{2+}]}{[NCaBD/Ca^{2+}][Ca^{2+}]} \quad (4)$$

The Eqs. 3 and 4 can be combined together to generate the Eq. 5.

$$NCaBD + 2\ Ca^{2+} \leftrightarrow NCaBD/2Ca^{2+} \qquad \beta_2 = \frac{[NCaBD/2Ca^{2+}]}{[NCaBD][Ca^{2+}]^2} = K_1 \times K_2 \quad (5)$$

Additional material

Additional file 1: Figure S1. Binding of Ca^{2+} to NCaBD as measured by ITC. For each injection, 4-μL of a 4-mM Ca^{2+} solution was mixed in a sample cell containing 0.155 mM NCaBD at 25°C. The corrected heats evolved per injection for N-CaBD was either fitted to a model with 2 independent binding sites (solid line) or with a model with identical, cooperative binding sites (dashed line).

Additional file 2: Figure S2. SDS-PAGE of purified proteins.

Abbreviations

AEDANS: *N*-(iodoacetyl)-*N* -(5-sulfo-1-napthyl)ethylenediamine; CaBD: Calcium binding domain; CaM: Calmodulin; CD: Circular dichroism; EDTA: Ethylenediaminetetraacetic acid; FAD: Flavin adenine dinucleotide; IPTG: Isopropyl-β-D-thiogalactopyranoside; ITC: Isothermal titration calorimetry; NADPH: Nicotinamide adenine dinucleotide phosphate; NCaBD: The N-terminal half of CaBD; NOX: NADPH Oxidase; OD: Optical density.

Acknowledgements

We thank Dr. Carl Frieden at Washington University in St. Louis (WUSTL) for allowing us to use his CD spectrometer. We also thank the internal financial supports from Southern Illinois University Edwardsville: Seed Grants for Transitional and Exploratory Projects (STEP) to CW; Research Grants for Graduate Students (RGGS) to NR; and Undergraduate Research and Creative Activities (URCA) assistantship to CP. This work was supported in part by Cottrell College Science Awards 7322 from Research Corporation and National Science Foundation grant DUE-0941517 to CW.

Author details

[1]Department of Chemistry, Southern Illinois University Edwardsville, Edwardsville, IL 62026, USA. [2]Department of Biological Sciences, Southern Illinois University Edwardsville, Edwardsville, IL 62026, USA. [3]Department of

Pathobiology, the Lerner Research Institute, Cleveland Clinic Foundation, Cleveland, OH 44195, USA. [4]Department of Chemistry, Kent State University at Tuscarawas, New Pheladelphia, OH 44663, USA.

Authors' contributions

NR and CP carried out recombinant protein expression and biochemical characterizations, KW and TB performed large scale protein expression and purification. YP and ZW carried out plasmid construction. All authors have read and approved the final manuscript.

Competing interests

The authors declare that they have no competing interests.

Received: 8 February 2012 Accepted: 10 April 2012
Published: 10 April 2012

References

1. Bedard K, Krause KH: **The NOX family of ROS-generating NADPH oxidases: physiology and pathophysiology.** *Physiol Rev* 2007, **87(1)**:245-313.
2. Lambeth JD, Kawahara T, Diebold B: **Regulation of Nox and Duox enzymatic activity and expression.** *Free Radic Biol Med* 2007, **43(3)**:319-31.
3. Cheng G, Cao Z, Xu X, van Meir EG, Lambeth JD: **Homologs of gp91phox: cloning and tissue expression of Nox3, Nox4, and Nox5.** *Gene* 2001, **269(1-2)**:131-40.
4. Nauseef WM: **Assembly of the phagocyte NADPH oxidase.** *Histochem Cell Biol* 2004, **122(4)**:277-91.
5. Tirone F, Radu L, Craescu CT, Cox JA: **Identification of the binding site for the regulatory calcium-binding domain in the catalytic domain of NOX5.** *Biochemistry* 2010, **49(4)**:761-71.
6. Banfi B, Tirone F, Durussel I, Knisz J, Moskwa P, Molnar GZ, Krause KH, Cox JA: **Mechanism of Ca2+ activation of the NADPH oxidase 5 (NOX5).** *J Biol Chem* 2004, **279(18)**:18583-91.
7. Wei C-C, Motl N, Levek K, Chen L-Q, Yang Y-P, Johnson T, Hamilton L, Stuehr DJ: **Conformational states and kinetics of the calcium binding domain of NADPH Oxidase 5.** *Open Biochem J* 2010, **4**:59-67.
8. Beckingham K: **Use of site-directed mutations in the individual Ca2 (+)-binding sites of calmodulin to examine Ca2(+)-induced conformational changes.** *J Biol Chem* 1991, **266(10)**:6027-30.
9. Freire E, Schon A, Velazquez-Campoy A: **Isothermal titration calorimetry: general formalism using binding polynomials.** *Methods Enzymol* 2009, **455**:127-55.
10. Brown A: **Analysis of cooperativity by isothermal titration calorimetry.** *Int J Mol Sci* 2009, **10(8)**:3457-77.
11. Gifford JL, Walsh MP, Vogel HJ: **Structures and metal-ion-binding properties of the Ca2 + -binding helix-loop-helix EF-hand motifs.** *Biochem J* 2007, **405(2)**:199-221.
12. Blanchard H, Grochulski P, Li Y, Arthur JS, Davies PL, Elce JS, Cygler M: **Structure of a calpain Ca(2+)-binding domain reveals a novel EF-hand and Ca(2+)-induced conformational changes.** *Nat Struct Biol* 1997, **4(7)**:532-8.
13. Lin GD, Chattopadhyay D, Maki M, Wang KK, Carson M, Jin L, Yuen PW, Takano E, Hatanaka M, DeLucas LJ, Narayana SV: **Crystal structure of calcium bound domain VI of calpain at 1.9 A resolution and its role in enzyme assembly, regulation, and inhibitor binding.** *Nat Struct Biol* 1997, **4(7)**:539-47.
14. Di Cera E: *Thermodynamic Theory of Site-Specific Binding Processes in Biological Macromolecules* Cambridge University Press: New York; 2005, 108-123.
15. Tochtrop GP, Richter K, Tang C, Toner JJ, Covey DF, Cistola DP: **Energetics by NMR: site-specific binding in a positively cooperative system.** *Proc Natl Acad Sci USA* 2002, **99(4)**:1847-52.
16. Tikunova SB, Black DJ, Johnson JD, Davis JP: **Modifying Mg2+ binding and exchange with the N-terminal of calmodulin.** *Biochemistry* 2001, **40(11)**:3348-53.
17. Tirone F, Cox JA: **NADPH oxidase 5 (NOX5) interacts with and is regulated by calmodulin.** *FEBS Lett* 2007, **581(6)**:1202-8.
18. Jagnandan D, Church JE, Banfi B, Stuehr DJ, Marrero MB, Fulton DJ: **Novel mechanism of activation of NADPH oxidase 5. calcium sensitization via phosphorylation.** *J Biol Chem* 2007, **282(9)**:6494-507.

doi:10.1186/1752-153X-6-29
Cite this article as: Wei *et al.*: Characterization of the 1st and 2nd EF-hands of NADPH oxidase 5 by fluorescence, isothermal titration calorimetry, and circular dichroism. *Chemistry Central Journal* 2012 **6**:29.